Chemical Engineering Journal 353 (2018) 727–735

Contents lists available at ScienceDirect

Chemical Engineering Journal

journal homepage: www.elsevier.com/locate/cej

Furfural degradation through heat-activated persulfate: Impacts of simulated brine and elevated pressures

Katherine E. Manz[a,b], Taylor J. Adams[b,c], Kimberly E. Carter[a,b,*]

[a] UT/ORNL Bredesen Center, University of Tennessee, Knoxville, TN 37996, USA
[b] Department of Civil and Environmental Engineering, University of Tennessee, Knoxville, TN 37996, USA
[c] Department of Chemical and Biomolecular Engineering, University of Tennessee, Knoxville, TN 37996, USA

HIGHLIGHTS

- Furfural degradation in lab simulated hydraulic fracturing brine with persulfate.
- Novel activation of persulfate using extreme pressures.
- Persulfate activation at borehole conditions including heat, varying pH, and iron.
- Identified reaction byproducts showed formation of halogenated organics in brine.

GRAPHICAL ABSTRACT

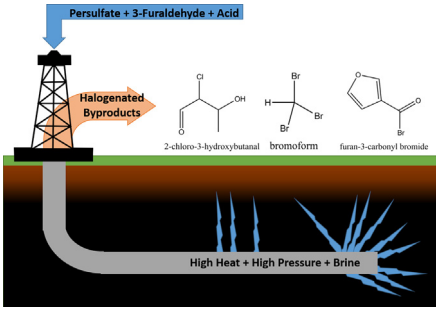

ARTICLE INFO

Keywords:
3-Furaldehyde
Heat-activated persulfate oxidation
Fe (III)
Hydraulic fracturing
High pressure
Halogenated organic byproducts

ABSTRACT

Persulfate is used as an oxidizing breaker in hydraulic fracturing fluids to breakdown gelling agents and clean out wellbores. Persulfate may be activated using conditions like those encountered in the wellbore, producing strong oxidizing radicals that degrade organic compounds. Thus, this study examined persulfate activated transformation of organic additives in a simulated hydraulic fracturing brine by investigating the transformation of furfural. Pseudo-first-order reactions kinetics of furfural degradation in conditions that mimic a fracture, including high temperature, acidified pH, ferric sulfate, and a laboratory simulated hydraulic fracturing brine, were established. The activation energies for furfural removal in acidic (pH 2.54) hydraulic fracturing brine was 105.6 kJ mol^{-1} without ferric sulfate and 105.1 kJ mol^{-1} with 23.3 mg L^{-1} ferric sulfate. A high-pressure reactor was used to simulate the effects of pressure on persulfate activation. Increasing pressure was shown to increase activation of persulfate at 55 °C. Applying 3000 psi to the reactor nearly halved the apparent furfural activation energy compared to experiments at atmospheric pressure. Finally, reaction byproducts were presented with the findings showing that halogenated organic byproducts form in hydraulic fracturing brine during persulfate use.

1. Introduction

Increasing population and energy production continue to place demands on water resources [1]. In response to the energy demand, the US has turned to natural gas, with most extraction achieved through hydraulic fracturing of unconventional reservoirs [2,3]. Hydraulic fracturing has become a public concern as industry practices have impacted the environment [4,5].

* Corresponding author at: Department of Civil and Environmental Engineering, University of Tennessee, Knoxville, TN 37996, USA.
E-mail address: kcarte46@utk.edu (K.E. Carter).

https://doi.org/10.1016/j.cej.2018.07.142
Received 7 May 2018; Received in revised form 19 July 2018; Accepted 21 July 2018
Available online 23 July 2018
1385-8947/

Adding chemical agents to the large quantities of water used to fracture a single well degrades the water quality, which then requires proper treatment or disposal [6,7]. In the Marcellus region alone, over 350 organic species have been reported by hydraulic fracturing companies [8]. Additives used depend on the day-to-day conditions of the well, but include surfactants, gelling agents, biocides, and breaking agents [9–12]. Chemical transformations occur because of high downhole temperatures and pressures; however, the reactions are different for each chemical agent [13,14]. For instance, breaking agents decompose target gelling agents to smaller molecular components to allow fluid and gas to return to the well surface. Enzyme breakers react with the gelling agent at specific sites, while non-selective, "delayed" breakers oxidize the nearest constituent. Furthermore, as the fluids extract materials from the geological formation, high inorganic salt concentrations, or total dissolved solids (TDS), are introduced to the mixture [4]. Sodium persulfate, a delayed breaker used in hydraulic fracturing [15], forms sulfate and hydroxyl radicals with activation by conditions encountered during a fracture, such as elevated temperature, acid addition, and iron concentrations as shown in Reactions (1) to (5) [9,16–22]. Persulfate concentration used may vary between 0.125 and 47 mmol L^{-1}, depending on the well location and formation conditions [9].

Little information on how high pressure influences the chemistry of hydraulic fracturing has been published. Previous studies have investigated the transformation of glutaraldehyde, an organic biocide used in hydraulic fracturing, under high pressure conditions [14]. Kahrilas et al. determined that high pressure did not impact the hydrolysis of glutaraldehyde [14]; however, the use of oxidizers was not considered in this study. Current studies that consider the use of oxidizers, such as persulfate, do not consider the high pressures reached in the well bore [9,11]. Under high pressure, oxidizers likely accelerate chemical transformation and the formation of unintended byproducts. When halogens, such as those contained in hydraulic fracturing brine or the shale rock, are present, reactions with persulfate may lead to the formation of halogenated organic byproducts, which have been detected in produced water [23]. Halogenated organic byproducts are regulated by the EPA as they are associated with cancer, birth defects, cytotoxicity, genotoxicity, and other adverse health effects [24–30].

In addition to increasing potential for halogenated organic byproduct formation, TDS (5000 mg L^{-1} to greater than 200,000 mg L^{-1}) [4,31–33] and brine content (32,000 to 148,000 mg L^{-1} chloride, 720 to 1600 mg L^{-1} bromide, and 9100 to 55,000 mg L^{-1} carbonate species) [4,34–37] in hydraulic fracturing wastewater varies between fractures and may scavenge radicals formed from persulfate activation, as shown in Reactions 6–11, requiring additional persulfate use [11,38–40]. Ions compete for the radicals, but the extent depends on pH [38,41]. Hydrochloric acid added by hydraulic fracturing companies [6,10,42,43] may increase radical quenching at low concentrations or decrease quenching at higher concentrations [17,44,45]. Additionally, downhole temperatures may reach 140 °C, which would rapidly activate persulfate and breakdown organic additives [46]. To date, the impact of extreme downhole pressures, which may exceed 6000 psi [46], on persulfate activation have not been investigated.

$$S_2O_8^{2-} \rightarrow 2SO_4^{\cdot -} \quad k_1 = 1.1 \times 10^8\ M^{-1}\ s^{-1} \tag{1}$$

$$S_2O_8^{2-} + Me^{n+} \rightarrow Me^{n+1} + SO_4^{\cdot -} + 2SO_4^{2-} \quad k_2 = 20\ M^{-1}s^{-1} \text{ for } Fe^{2+} \tag{2}$$

$$S_2O_8^{2-} + Me^{n+1} \rightarrow Me^{n+} + S_2O_8^{\cdot -} \tag{3}$$

$$S_2O_8^{2-} + H^+ \rightarrow HS_2O_8^- \tag{4}$$

$$HS_2O_8^- \rightarrow H^+ + SO_4^{\cdot -} + SO_4^{2-} \tag{5}$$

$$SO_4^{\cdot -} + Cl^- \rightarrow SO_4^{2-} + Cl^{\cdot} \quad k_6 = 2.5 \times 10^8\ M^{-1}\ s^{-1} \tag{6}$$

$$Cl^{\cdot} + H_2O \rightarrow ClHO^{\cdot -} + H+ \quad k_7 = 1.3 \times 10^3\ M^{-1}\ s^{-1} \tag{7}$$

$$ClHO^{\cdot -} \rightarrow HO^{\cdot} + Cl^- \quad k_8 = 4.3 \times 10^9\ M^{-1}\ s^{-1} \tag{8}$$

$$SO_4^{\cdot -} + HCO_3^- \rightarrow SO_4^{2-} + HCO_3 \quad k_9 = (1.6 \pm 0.2) \times 10^6\ M^{-1}\ s^{-1} \tag{9}$$

$$HCO_3^- \rightarrow H^+ + CO_3^- \tag{10}$$

$$SO_4^{\cdot -} + CO_3^{2-} \rightarrow SO_4^{2-} + CO_3^- \quad k_{11} = (6.1 \pm 0.4) \times 10^6\ M^{-1}\ s^{-1} \text{ at } pH > 11 \tag{11}$$

The objective of this study is to determine the impacts elevated pressures and the presence of TDS has on furfural degradation and formation of transformation byproducts in laboratory simulated hydraulic fracturing brine. The chemical changes that occur over the course of a fracture were investigated using one model additive, 3-furfuraldehyde or "furfural" (a component of an enzyme breaker called "LEB-10X" and proppant material), and a laboratory composed hydraulic fracturing brine [9,12,47,48]. Extreme pressures were studied by observing changes in furfural degradation rates and transformation byproducts using persulfate in the brine. Conditions used in this study, including temperature, pressure, persulfate concentration, brine content, pH, and iron concentrations, were used to simulate those experienced during the hydraulic fracturing process [9].

2. Experimental

2.1. Chemicals

All solutions were prepared using deionized water produced by a Milli-Q Plus water purification system (Darmstadt, Germany). 3-furladehyde or furfural was purchased from Sigma Aldrich (St. Louis, MO 63103). Optima grade hexane and 97% tribromomethane stabilized with ethanol were purchased from Fisher Scientific (Pittsburgh, PA 15275, USA). Inorganic salts, aluminum sulfate ($Al_2(SO_4)_3$) (> 99%), ferric sulfate ($Fe_2(SO_4)_3$) (99%), hydrochloric acid (HCl), potassium bromide (KBr) (> 99%), potassium chloride (KCl) (99%), potassium sulfate (K_2SO_4) (99%), sodium bicarbonate ($NaHCO_3$) (> 99%), sodium hydroxide (NaOH), sodium persulfate ($Na_2S_2O_8$) (> 98%), sodium chloride (NaCl) (> 99%), and potassium iodide (KI) (> 99%) were purchased from Fisher Scientific (Pittsburgh, PA 15275, USA). LEB-10X, an enzyme breaker, and WGA, a gelling agent, were obtained from Weatherford International (Houston, Texas, USA).

2.2. Batch oxidation experiments at ambient pressure

Solutions containing 120 mg L^{-1} (1.25 mmol L^{-1}) furfural and hydraulic fracturing brine were prepared 24 h prior to starting the experiments. Furfural is used in hydraulic fracturing additive LEB-10X, an enzyme breaker, which are used in concentrations ranging from 1 to 400 mg L^{-1} [6,9]. Based on this value, the concentration of furfural in the fluids will be less than 400 mg L^{-1} and 120 mg L^{-1} was used in these experiments for ease of measurement. Hydraulic fracturing brine solution was composed of 1 g L^{-1} (17.1 mmol L^{-1}) sodium chloride, 20 mg L^{-1} (0.27 mmol L^{-1}) potassium chloride, 25 mg L^{-1} (0.14 mmol L^{-1}) potassium sulfate, 15 mg L^{-1} (0.13 mmol L^{-1}) potassium bromide, 15 mg L^{-1} (0.18 mmol L^{-1}) sodium bicarbonate, and 15 mg L^{-1} (0.044 mmol L^{-1}) aluminum sulfate [49]. Iron activation of the persulfate was performed by adding 23.3 mg L^{-1} (0.058 mmol L^{-1}) ferric sulfate to the brine. pH was adjusted to 2.54 using 0.07% hydrochloric acid, to achieve acidic conditions used in the industry, and measured with Fisher Scientific Accumet XL600 benchtop pH meter (Pittsburgh, PA 15275, USA) [6,50,51].

Batch experiments were performed in triplicate using 100-mL volumes in 125-mL amber borosilicate volatile organic carbon jars closed with Teflon-lined screw caps. Jars were placed in a shaking water bath at 20, 30, 40, 55, or 60 °C 12 h prior to experiment start. To initiate

experiments, solutions were spiked with a 1050 mmol L^{-1} stock sodium persulfate solution to reach concentrations of 0.6, 5, 10, 15, and 21 mmol L^{-1}. Stock persulfate solutions were prepared and mixed within 1 h of starting experiments. Experiments were carried out for 8 h. 4.5-mL samples were taken at time intervals of 0, 15, 30, 60, 120, 240, 360 and 480 min. Mass balance calculations were performed to minimize sampling effects. Samples were pipetted into Eppendorf tubes, placed in an ice bath (4 °C) to quench the persulfate reactions, and analyzed within 2 h of collection [9,52–54].

2.3. Oxidation experiments at elevated pressure

High pressure experiments were conducted using an extra capacity high pressure generator (Model 112-5.75-5) connected to a 500-mL stainless steel reactor with an O-ring seal (Model OC-9) (High Pressure Equipment Company, Erie, PA 16505). Reactor set-up is illustrated in SI (Figs. S1 and S2). Reactor temperature was controlled using a custom-made silicone impregnated fiberglass heating jacket equipped with a programmable temperature controller (HTS/Amptek, Stafford, TX 77497). The temperature was set at least 36 h prior to beginning the experiment to allow for temperature stabilization.

The degradation of persulfate in DI water was investigated at 14.7, 1000, 2000, 3000 and 4000 psi. The temperature jacket was set to a constant temperature of 58 °C. Samples were taken at 0, 5, 15, 20, 25, 30, 40, 50, 60 75, 90, 105, and 120 min. A reservoir was used to feed the reactor DI water, which is required to build pressure in the reactor. During sample collection, 5-mL sample volumes were replaced with the DI water from the feed reservoir. Mass balance calculations were performed to account for changes in persulfate concentration caused by dilution with the DI feed solution.

3-Furaldehyde degradation by pressure activated persulfate experiments were performed at 14.7 psi and 3000 psi. A reservoir was used to feed the reactor a concentrated solution of 128 mM sodium persulfate. During sample collection, 20-mL sample volumes were replaced with the stock persulfate solution ensuring a constant 5.12 mM persulfate concentration inside the reactor. Samples were taken at 0, 5, 15, 20, 25, 30, 40, 50, 60 75, 90, 105, and 120 min. Experiments performed at 20 °C were extended to 2400 min due to slow persulfate activation at this temperature. Mass balance calculations were performed to account for changes in furfural concentration caused by dilution with the persulfate stock solution. Experiments performed with hydraulic fracturing additives LEB-10X (0.025 gallons per 1000 gallons of water) and WGA (25 gallons per 1000 gallons of water) were added in concentrations for typical use indicated by the chemical supplier.

2.4. Sample analysis

Furfural matrix (furfural and degradation byproducts) and persulfate concentrations were determined using UV/Vis spectrophotometry (Thermo Fisher Scientific, Evolution-600 Madison, WI 53711, USA). Furfural absorbance was evaluated at the maximum wavelength (258-nm) [55–57]. Calibration curves were used to determine furfural concentration and made through serial dilutions of known furfural concentration stock solution. A modified spectrophotometric/iodometric method previously described by the authors was used to determine persulfate concentration (352-nm maximum UV-vis wavelength) [9,58]. Experiments were performed in triplicate; thus error bars represent standard error [49].

2.5. Reaction byproducts analysis

3-mL samples were extracted using liquid-liquid extraction with 3-mL hexane, dichloromethane, toluene, or ethyl acetate as previously described [9,49]. Extractants were analyzed using an Agilent 7890B gas chromatograph (GC) equipped with a DB-1 capillary column (30-m × 0.25-mm inner diameter × 0.25-μm film thickness) and a 5977A Mass Selective Detector (MS) (Santa Clara, CA 95051, USA). Ultra-high purity helium was the carrier gas and maintained at 1.5 mL min^{-1} (Airgas Corporation, Knoxville, TN 37921, USA). The GC/MS was operated in split-less mode with a sample injection volume of 2-μL. An initial temperature of 40 °C was held for 2 min prior to and after a temperature ramp of 2.5 °C/min to 100 °C. NIST11 mass-spectral library database was used for substance identification of gas chromatogram peaks.

2.6. Kinetics

Overall pseudo first-order rate constants for furfural removal and furfural half-lives were determined assuming irreversible first-order kinetics [59,60]. Overall pseudo first-order rate constants (k_{obs}) were calculated using Eq. (1), where C is the furfural concentration at a specific time, t. Furfural half-lives were calculated using Eq. (2). Reaction rate constants were plotted against inverse temperature (T, °K) to determine apparent furfural degradation activation energy (E_a), which was calculated using Eq. (3), where R is the universal gas constant. Under the assumption that the activation energies for furfural degradation by each individual radical produced by persulfate have similar activation energies, the calculated activation energy will be referred to as the "apparent activation energy for furfural degradation" and is the amount of energy required for the parallel radical reactions degrading furfural and the temperature dependency of persulfate decomposition to the radicals [61].

$$\ln\left(\frac{C}{C_o}\right) = k_{obs} * t \tag{1}$$

$$t_{\frac{1}{2}} = \frac{\ln(2)}{k_{obs}} \tag{2}$$

$$k_{obs} = A * e^{\frac{-Ea}{RT}} \tag{3}$$

3. Results and discussion

3.1. Temperature dependence at atmospheric pressure

Fig. S3 (SI) shows furfural stability in pH 2.54 hydraulic fracturing brine with and without ferric sulfate at 20 °C (no sodium persulfate). As observed in Fig. S3, without persulfate addition, furfural concentration decreased by 3.3% and 6.5% without ferric sulfate and with 23.3 mg L^{-1} ferric sulfate, respectively, over the course of 480 h. Furfural is more persistent in the hydraulic fracturing fluid environment with a half -life of 188 ± 7.19 days in pH 2.54 brine without ferric sulfate compared to the furfural half-life in water (84.7 days) [9]. Additionally, the furfural half-life increased to 199 ± 7.67 days in brine containing 23.3 mg L^{-1} ferric sulfate. The increased furfural half-life in these solutions suggests that inorganic salts and acidic conditions found in hydraulic fracturing fluids may increase persistence of certain organics by preventing hydrolysis [62–64].

Persulfate use in hydraulic fracturing fluids may cause organic species concentration to decrease via oxidation. Fig. S4 (SI) displays furfural degradation using 21 mmol L^{-1} persulfate in hydraulic fracturing brine (pH 2.54) with 0 and 23.3 mg L^{-1} ferric sulfate at 20 °C. When 21 mmol L^{-1} persulfate was added, furfural concentration decreased more rapidly as shown in Fig. S4, which is expected because, while slow, direct reaction with persulfate degrades contaminants in solution [65]. After 289 h, furfural concentration decreased by 81.3% without ferric sulfate in the brine and by 90.1% with 23.3 mg L^{-1} ferric sulfate. The 9% difference in furfural removal may be due to persulfate activation by the iron species present [9].

Fig. S5 displays the natural log of C_t/C_o as a function of time for the 20 °C data, which was used to determine the pseudo-first-order reaction rate constants for these reactions. Table S1 (SI) displays the pseudo-

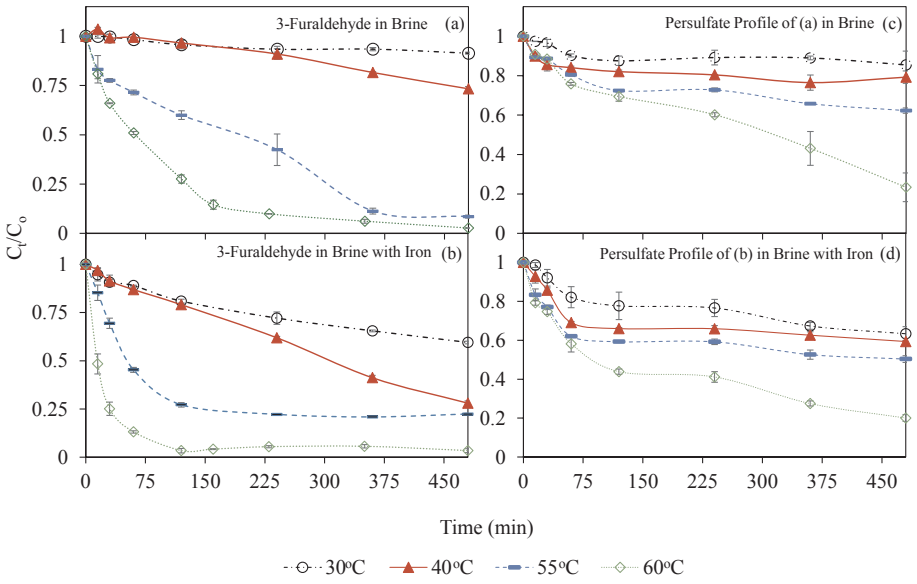

Fig. 1. Furfural removal in pH 2.54 hydraulic fracturing brine with a) 0 and b) 23.3 mg L^{-1} ferric sulfate at different temperatures (21 mmol L^{-1} sodium persulfate dosage). Parts c) and d) display the persulfate profiles for a) and b), respectively. Error bars represent standard error.

first-order reaction rate constants for all batch experiments performed in hydraulic fracturing brine. With ferric sulfate, a higher reaction rate constant was achieved because iron activation of persulfate leads to the formation of stronger oxidizing sulfate radicals [20]. Compared to previous experiments without brine [9], it appears that at 20 °C the brine has a quenching effect on furfural removal only when iron is present at this temperature. When iron is not present, furfural degradation in hydraulic fracturing brine occurred more rapidly compared to when iron was present. Ferric sulfate activates persulfate very rapidly, encouraging scavenging radical-to-radical and radical-to-anion reactions to occur in place of radical-to-furfural reactions [38]. Furthermore, concentrations of chloride up to 28 mM, which is greater than this study's brine, and between 10 and 100 mM have shown to enhance degradation via persulfate [41,45].

Fig. 1 displays decreasing furfural concentration caused by persulfate oxidation (21 mmol L^{-1} sodium persulfate dose) during the 480-minute experiments in hydraulic fracturing brine (pH 2.54) at elevated temperatures (30, 40, 55 and 60 °C). Data for the 0 and 23.3 mg L^{-1} ferric sulfate are displayed in Fig. 1a and b, respectively. Fig. 1c and d show the persulfate profiles for furfural degradation in simulated brine and simulated brine with iron, respectively. As temperature increases, greater furfural removal is achieved in less time in hydraulic fracturing brine regardless of the ferric sulfate presence. Similarly, greater decrease in persulfate concentration is observed as temperature increases regardless of the presence of ferric sulfate. This was an expected result as previous studies have shown that persulfate can be activated at temperatures greater than 30 °C to produce strong oxidizing radicals [20,65]. Without ferric sulfate at 60 °C in hydraulic fracturing brine (pH 2.54), 97% furfural removal is achieved after 480 min; however, with ferric sulfate, 97% furfural removal is achieved after 120 min. The shorter time for the same removal of furfural is due to the additional persulfate activation by iron. The overall furfural degradation reaction with persulfate is shown in Reaction 12. The reaction is used to indicate the stoichiometry for the furfural reaction with persulfate. For each mole of furfural degraded, 10 mol of persulfate are required. Thus, the 21 mmol of persulfate is sufficient for degrading the 1.25 mmol of furfural in these experiments. Using reaction 12, the stoichiometric efficiency may also be calculated by dividing the number of moles of furfural degraded by the number of moles persulfate consumed for the 480-minute reaction period [66]. Without iron, the reaction stoichiometric efficiencies for 30, 40, 55, and 60 °C were 1.65, 7.65, 15.0, 7.56%, respectively. With 23.3 mg L^{-1} ferric sulfate, the reaction stoichiometric efficiencies for 30, 40, 55, and 60 °C were 4.93, 11.3, 11.2, 6.35%, respectively. At lower temperatures, the reaction stoichiometric efficiencies improved with the addition of iron. At higher temperatures, the reaction efficiencies decreased with the iron addition.

$$C_5H_4O_2 + 10S_2O_8^{2-} + 8H_2O \rightarrow 5CO_2 + 20HSO_4^- \quad (12)$$

Natural log of C_t/C_o as a function of time for these experiments are displayed in Fig. 2. As expected, increasing temperatures resulted in increasing reaction rate constants. In Fig. 2, degradation of 3-furaldehyde in hydraulic fracturing brine appears to have two-phases of degradation. Initially, furfural degrades very rapidly (within the first 75 min) at 55 and 60 °C. However, degradation appears to slow down after 75 min at the higher temperatures. In the first phase of degradation, furfural is more abundant and the persulfate is able to degrade the furfural. As displayed in Fig. 1c and d, after 75 min, the activation of persulfate also slows down. This coincides with the slowed furfural degradation at 30, 40 and 55 °C compared to the data at 60 °C. This could be due to the production of byproducts that scavenge the persulfate or sulfate radicals. In the case of the brine solution, furfural degradation is fast in the beginning but then slows down. This may be due to the ions in the simulated brine, such as chlorine and carbonate, that are now in a higher abundance than the furfural, and their impact on sulfate radical scavenging is more pronounced [38]. The chlorine and carbonate radicals produced in Reaction 6, 7 and 9 will react slower than persulfate or hydroxyl radicals, causing the slowing of the furfural degradation.

Fig. 2(c) displays plots of natural log of k_{obs} vs. 1/T for the same experiments with varying temperature in pH 2.54 hydraulic fracturing brine with 0 and 23.3 mg L^{-1} ferric sulfate (21 mmol L^{-1} sodium persulfate dose) and Table S2 (SI) displays the resulting parameters. While very different pseudo-first-order reaction rate constants and furfural removals were achieved for the solutions with and without ferric sulfate, the apparent furfural removal activation energy was not affected as displayed in Fig. 2(c) and Table S2. Apparent activation energy for furfural removal in acidic hydraulic fracturing brine was 105.6 kJ mol^{-1} without ferric sulfate and 105.1 kJ mol^{-1} with 23.3 mg L^{-1} ferric sulfate. These values are less than 2.5% different from previously reported activation energies for furfural removal (107 kJ mol^{-1}) in neutral water, but are 30% different from activation energy for furfural removal in pH 2.54 water (75 kJ mol^{-1}) [9]. The

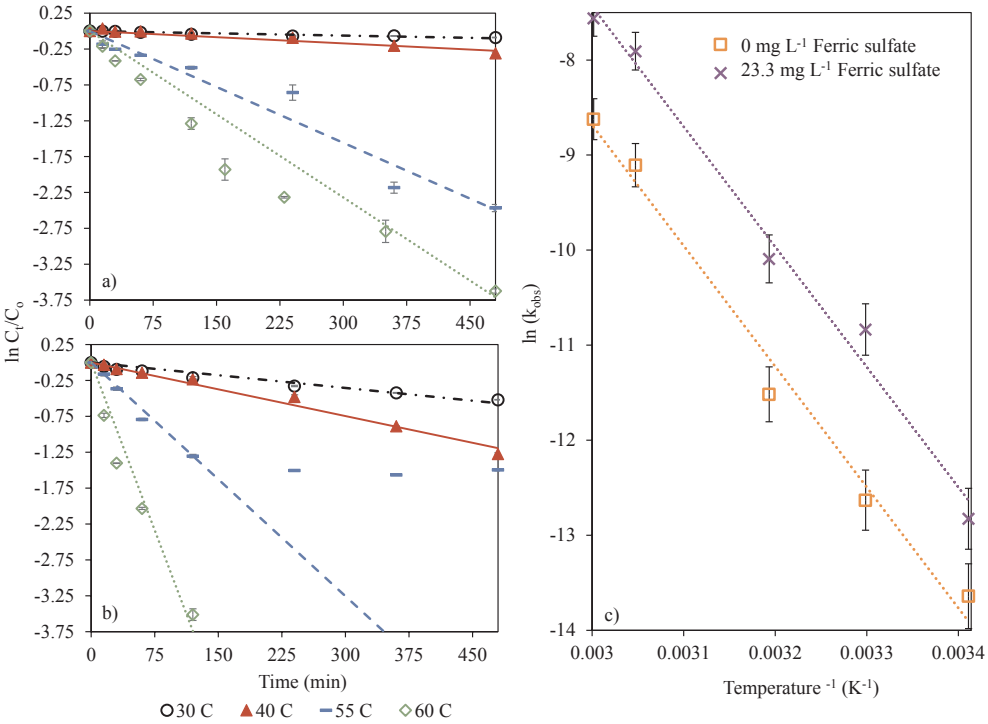

Fig. 2. Pseudo-first-order natural log versus time plots for decreasing furfural concentration in pH 2.54 hydraulic fracturing brine at 30, 40, 55 and 60 °C (21 mmol L^{-1} initial sodium persulfate dosage). Experiments with (a) 0 and (b) 23.3 mg L^{-1} ferric sulfate. The resulting Arrhenius plots are shown in (c) for furfural degradation in pH 2.54 hydraulic fracturing brine with 0 and 23.3 mg L^{-1} ferric sulfate (pH 2.54, initial sodium persulfate dose of 21 mmol L^{-1}). Error bars represent standard error.

furfural activation energy difference between the acidified brine and acidified water is likely due to the high TDS content in the brine. The anions in the brine impede persulfate oxidation by scavenging the radicals in solution [67,68]. The degree of quenching observed in hydraulic fracturing fluids depends on the temperature conditions downhole [16,20,69]. At higher temperatures, such as 100 °C, the quenching reactions by ions have more enhanced scavenging effects compared to scavenging effects at lower temperatures, such as 20 °C – meaning that at high temperatures a lower concentration of ions is required to quench reactions [20]. Hydraulic fracturing brine has a quenching effect on furfural removal at the elevated temperatures tested in this study. The difference in furfural activation energy between acidified brine and acidified water suggests hydraulic fracturing fluid conditions activate persulfate and encourage radical-to-anion reactions to occur in place of some radical-to-furfural reactions.

3.2. Initial pH dependence at atmospheric pressure

Fig. S6 (SI) displays the decrease in furfural concentration in simulated hydraulic fracturing brine containing 23.3 mg L^{-1} ferric sulfate with an initial unadjusted pH (initial pH 5.4) and with 0.07% hydrochloric acid added (pH 2.54) with persulfate dosages of 5, 10, and 15 mmol L^{-1} at 55 °C. Previous control studies demonstrated that furfural and iron do not coagulate or precipitate at the pHs and concentrations tested in this study [9]. At low pHs, furfural degradation occurs rapidly at all three persulfate doses compared to neutral pH. As shown in Fig. S6b, at pH 2.54, 93% furfural removal was observed after 480 min for all three sodium persulfate dosages. Within 120 min, 84% degradation was achieved when the sodium persulfate dosages were 10 and 15 mmol L^{-1}. A 75% decrease in furfural concentration is observed for the 5 mmol L^{-1} persulfate dose. Throughout the experiments, the largest difference in furfural concentration that occurred at any one time was 9% for the three sodium persulfate dosages at pH 2.54 and with 23.3 mg L^{-1} ferric sulfate. The data shows similar furfural degradation was achieved despite the initial sodium persulfate dosages in acidic brine containing 23.3 mg L^{-1} ferric sulfate.

At initial pH 5.4, greater differences between furfural degradation with varying persulfate dosages were observed. The final observed degradation with initial pH 2.54 brine with 23.3 mg L^{-1} ferric sulfate for 5, 10, 15 mmol L^{-1} sodium persulfate dosages were 85, 89, and 95%, respectively, after 480 min. After 120 min, 10, 21, and 32% furfural was removed with 5, 10, and 15 mmol L^{-1} sodium persulfate, respectively. The furfural removal was more gradual at the initial pH 5.4 than when initial pH was 2.54, thus the initial pH impacts furfural degradation through persulfate with brine present. Low pH increased the furfural degradation for all persulfate doses when brine contained iron, as acidic conditions lead to faster radical production [9,52]. Acidic pH has been shown to decrease the activation energy required to activate persulfate [18]. By decreasing the energy required for persulfate activation, the reaction may proceed faster, enabling faster removal of furfural. During furfural degradation, as carbon dioxide is produced, pH decreases and the effects of the acid presence may increase.

3.3. Influence of initial persulfate dose and ferric sulfate presence at atmospheric pressure

Fig. S7 (SI) displays decreasing furfural concentration with five initial persulfate dosages (0.6, 5, 10, 15, and 21 mM), at 55 °C in pH 2.54 simulated brine. Fig. S7a displays furfural removal over time without ferric sulfate and Fig. S7b and c display the removal with 23.33 mg L^{-1} ferric sulfate. Without ferric sulfate, more furfural degradation is achieved with higher sodium persulfate dosages in shorter time periods as more oxidizer is present in solution at any one time. After 480 min 95% furfural degradation was achieved with higher sodium persulfate dosages (10, 15, and 21 mM). With 23.33 mg L^{-1} ferric sulfate, furfural removal with each persulfate dose is less distinct. In simulated hydraulic fracturing brine, the furfural removal is less distinct because furfural is not the only constituent in the solution. The iron activates the persulfate very rapidly, but the brine also contains chloride and bicarbonate ions that have been shown to quench persulfate reactions. Chloride and bicarbonate limit the reactivity of sulfate radicals [70]. Rather than reacting with the furfural, the sulfate radicals may be scavenged by other ions in solution.

Fig. S8 (SI) shows the relationship between observed pseudo-first-order reaction rate constant and persulfate dose. Generally, higher persulfate doses led to higher pseudo-first-order reaction rate constants

as displayed in Fig. S8 (SI). Despite the presence of hydraulic fracturing brine, which contains persulfate reaction quenchers, the pseudo-first-order reaction rate constant increases linearly with persulfate dosing when no ferric sulfate is present. In more concentrated brines, it is expected that more quenching of persulfate or hydroxyl radicals would be observed, while higher temperatures will lead to faster activation. With iron present, the data is linear in the range of 0.6–15 mM persulfate ($R^2 = 0.98$ in this region); however, with 21 mM persulfate, the rate constant does not increase any further and is no longer linear. Iron activates persulfate more rapidly than heat alone and the radicals produced could be quenched by the ions, including iron, in solution. Nevertheless, the ferric sulfate concentration in hydraulic fracturing waters and the shale formation should be considered when adding persulfate for reuse and recycling or for cleaning out wells as it considerably impacts activation rate even when other ions are present.

3.4. Persulfate consumption in simulated hydraulic fracturing brine

Fig. S9 (SI) shows the decreasing persulfate concentration during experiments with varying persulfate doses (pH 2.54 brine, 0 and 23.3 mg L^{-1} ferric sulfate). Over the 480 min, persulfate was completely consumed when the initial dose was 0.6 mM in hydraulic fracturing brine with and without ferric sulfate. The two other cases where persulfate was consumed completely was when the initial dose was 5 and 10 mM in brine containing ferric sulfate. When persulfate remains in solution, furfural continually degrades. Furfural degradation was likely due to the radicals formed by chain reactions of the sulfate or hydroxyl radical produced by persulfate activation [17]. The by-products (discussed later), suggest that halogen radicals form in hydraulic fracturing brine and contribute to furfural removal [68,71]. In solutions containing ferric sulfate, more persulfate is consumed. Ferric sulfate and radical scavengers in hydraulic fracturing waters may prevent gelling agent breakdown by consuming the persulfate or radicals formed [9].

3.5. Persulfate activation through pressure elevation

Fig. 3a displays the degradation of persulfate in DI water at 58 °C at pressures of 14.7, 1000, 2000, 3000, and 4000 psi. As pressure increases, persulfate degrades faster. At 14.7 psi, the resulting reaction rate constant was 6.85×10^{-6} s^{-1} after mass balance calculations. This value is in agreement with values previously reported by House (4.55×10^{-6} s^{-1} at 56 °C and 8.03×10^{-6} s^{-1} at 60 °C) [18]. As displayed in Fig. 3b, between 14.7 and 4000 psi, the persulfate degradation rate constant increases linearly within this range ($R^2 = 0.975$). This demonstrates that pressure can influence persulfate activation and the reaction kinetics, but does not necessarily change the reaction mechanism. The autoionization of water is shown in Reaction 13. As temperature increases, the water autoionization constant, K_w, decreases, indicating an endothermic reaction [72–75]. Furthermore, as pressure increases, K_w, decreases. Because autoionization is favored at high temperature and pressure, H_3O^+ and OH^- become more dominant in solution [75]. The increased abundance of H^+ can cause the persulfate in solution to form $HS_2O_8^-$, as described in Reaction 4, which may produce more sulfate radicals as described in Reaction 5. It is important to note that since K_w decreases, the pH scale is also impacted; however, $[H_3O^+]$ and $[OH^-]$ are equal at neutral pH. Therefore, as $[H_3O^+]$ increases, $[OH^-]$ decreases, potentially causing more persulfate to activate. Persulfate activation through OH^- may occur after the persulfate has been activated by heat (Reaction (1) and sulfate radicals are in solution. The sulfate radicals may react with OH^- to produce hydroxyl radicals (Reaction 14), which can in turn, react with persulfate (Reaction 15) causing the decrease in concentration [52,76].

$$\text{heat} + H_2O \rightarrow H_3O^+ + OH^- \quad (13)$$

$$SO_4^{\cdot -} + OH^- \rightarrow SO_4^{2-} + OH^{\cdot} \quad (14)$$

$$OH^{\cdot} + S_2O_8^{2-} \rightarrow OH^- + S_2O_8^{\cdot -} \quad (15)$$

3.6. Degradation of 3-furaldehyde through pressure activated persulfate

Furfural removal in hydraulic fracturing brine (pH 2.54) over time is displayed in Fig. 4 at (a) ambient pressure and (b) 3,000 psi applied pressure at different temperatures. Fig. S10 and Fig. S11 (SI) show 20 °C data at both pressures over a longer time scale and the complete data set for 3000 psi experiments, respectively. As in the batch oxidation experiments, furfural degradation rate increased as temperatures increased. Due to difficulty in controlling the exact setting of internal reactor temperature, comparisons of exact same temperatures at atmospheric and elevated pressure were not achieved. Therefore, reaction rate constants and furfural removal achieved cannot be directly compared. However, resulting reaction rate constants, which are displayed in Table S3 (SI), may be compared in an Arrhenius plot, as shown in Fig. 5(c), to observe the difference in activation energy. The expressed activation energy is the effective activation energy and refers to the amount of energy required for the parallel reactions that occur to degrade furfural by all the potential radicals produced with the assumption that individual activation energies are not wide spread [61]. In reactor experiments performed without applied pressure, the apparent activation energy was 98.8 kJ mol^{-1} and the collision factor was 5.97×10^{13} ($R^2 = 1.00$). With 3000 psi applied, the apparent activation energy was 70.6 kJ mol^{-1} and the collision factor was 8.58×10^8 ($R^2 = 0.99$). The difference between the apparent activation energies suggests that increasing the pressure promotes furfural removal through persulfate activation and formation of radical species. If persulfate activation is not achieved due to lack of high temperatures in the wellbore, the extreme presssures exhibited during the hydraulic fracturing process may activate persulfate.

3.7. Degradation of 3-furaldehyde in presence of additives WGA and LEB-10X at high pressure

Furfural concentrations were also traced in the pressence of LEB-

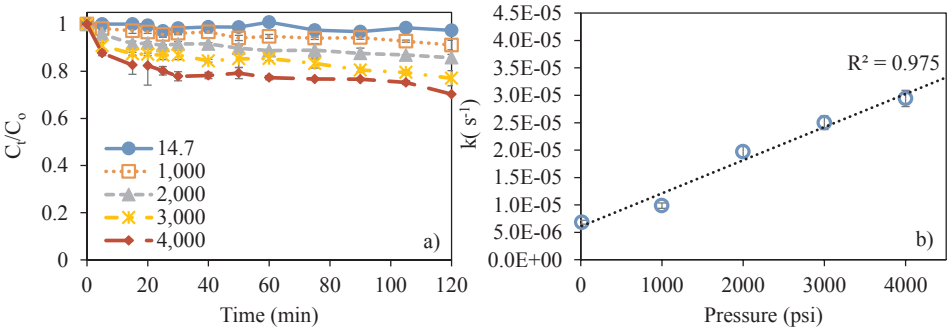

Fig. 3. Persulfate degradation in DI-water at 58 °C over time at varying pressure is displayed in (a). Persulfate degradation was observed at atmospheric pressure, 1000 psi, 2000 psi, 3000 psi, and 4000 psi. The relationship between the pseudo first order reaction rate constant and pressure is displayed in (b). In both, error bars represent standard error.

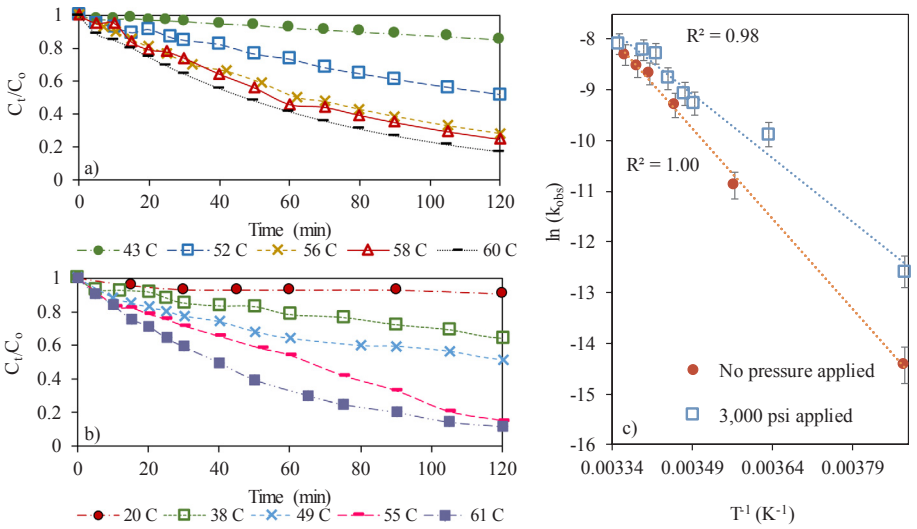

Fig. 4. Furfural removal in simulated brine over time in the high-pressure reactor (a) without pressure (14.7 psi) and (b) with 3000 psi applied. Arrhenius plots are shown in (c) and were used to determine activation energy for furfural removal without pressure (14.7 psi) and with 3000 psi applied to the reactor. Error bars in (c) represent 95% confidence interval.

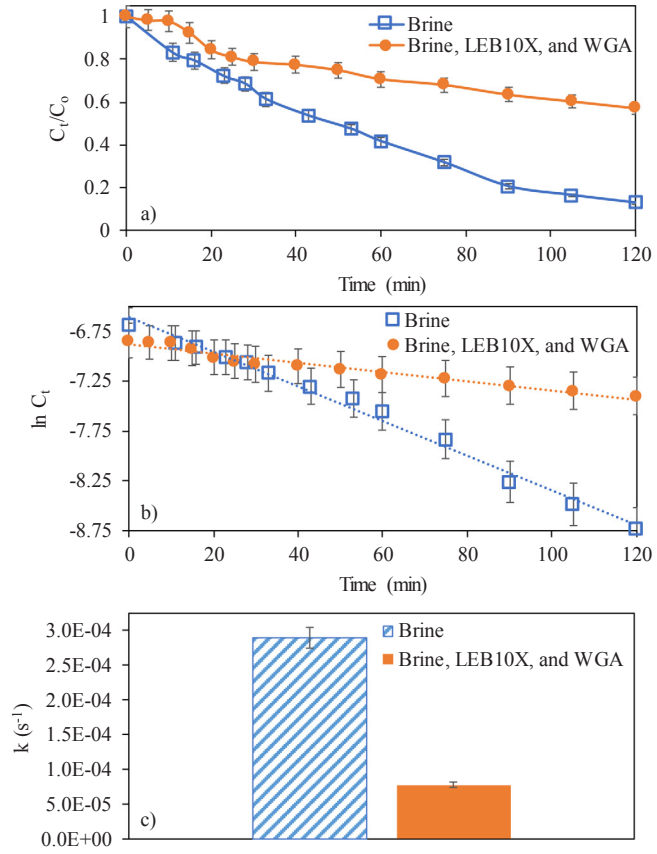

Fig. 5. Furfural degradation in simulated brine and simulated brine with chemical additives LEB10X and WGA (3000 psi applied to the reactor, 57 °C, pH 2.54, 23.3 mg L^{-1} ferric sulfate). Part a) shows the decrease in furfural concentration, b) shows the pseudo-first-order natural log of concentration versus time, and c) shows the difference in reaction rate constant. Error bars represent the 95% confidence interval.

10X, a hydraulic fracturing enzyme breaker, and WGA, a cellulosic gelling agent, at high pressure. The contents of LEB-10X have previosuly been analyzed using GC/MS and are presented in previous studies [9]. Fig. 5a displays the furfural concentration profile in brine containing LEB-10X and WGA at 57 °C and 3000 psi applied to the reactor (pH 2.54, 23.3 mg L^{-1} ferric sulfate). As shown in this figure, the presence of these additives prevented the degradation of furfural. After 120 min, almost 90% of furfural is degraded without the additives present. With LEB-10X and WGA, just 40% of the furfural is degraded after 120 min. Fig. 5b shows that the kinetics followed psuedo-first-order kinetics and Fig. 5c shows the resulting reaction rate constants for these reactions. The addition of the hydraulic fracturing additives decreased the reaction rate constant by 75%. As previously reported, persulfate attacks the furfural and the other components in the hydraulic fracturing fluids. These components can include target components, such as the gelling agent [9]. The results in this study indicate that the preference of persulfate to break down fluid components other than the target gelling agent still exists at high pressure.

3.8. Reaction byproducts

Furfural oxidation through activated persulfate in hydraulic fracturing brine produced byproducts previously reported when brine is not present [9], as well as several additional compounds. Previously reported byproducts include 3-methylbutanoic acid, (tetrahydrofuran-3-yl)methanol, tetrahydrofuran-3-carboxylic acid, 3-furancarboxylic acid, tetrahydrofuran-3-carboxylic acid, 2-ethylpropane-1,3-diol, and 2-methylbutanol [9]. Mass-spectra used to identify these compounds are shown in Fig. S11 (SI). Possible formation pathways have been previously discussed [9].

The additional reaction byproducts detected in the brine were halogenated organic byproducts. Fig. S12 displays their mass-spectra. The brine used in this study had low halogen ion concentration compared to concentrations observed in flowback or produced water samples [4,49,77,78]. However, even at low concentration, the halogenated organic byproducts formed were detected using GC/MS and include bromoform, 5-bromofuran-3-carbaldehyde, 3-bromofuran, 2-chloro-3-hydroxybutanal, ethylmethyl acetyl chloride, and 2-chloro-2-methyl propanal. At 3000 psi, two additional byproducts were detected, furan-3-carbonyl bromide and methyl monobromoacetate. Due to availability of standards, bromoform was the only compound confirmed.

Of these halogenated compounds, bromoform is the only one detected in produced waters [23]. As brominated organics are considered more toxic than their chlorinated analogs and bromoform is regulated by the EPA in drinking water [23,79], bromoform presence was verified by comparing against a bromoform standard. The standard's mass-spectrum compared to the experimental sample are shown in Fig. S14 (SI). Formation of the detected halogenated organic byproducts stem from rapid radical-to-halogen reaction with subsequent attack on furfural or any one of the degradation byproducts. The radicals, sulfate or hydroxyl, that propagate these chain reactions are present due to sodium persulfate addition. Once a radical is generated from persulfate,

the radical can initiate chain reactions, leading to formation of halogenated organic byproducts.

4. Conclusions

In this study, furfural degradation using activated persulfate in hydraulic fracturing brine was examined. Activation was achieved by conditions that occur during a fracture, including acidification with 0.07% hydrochloric acid, temperature increase, ferric sulfate addition, and elevated pressure. Despite presence of persulfate-quenching ions, furfural degraded in hydraulic fracturing brine. Moreover, in acidified brine with ferric sulfate, which mimics conditions observed during the hydraulic fracturing process without wellbore pressures, furfural transformed rapidly and the transformation extent was not dependent on persulfate dose.

The changes in reaction byproducts formed in the simulated hydraulic fracturing brine have important significance for handling hydraulic fracturing fluids post-injection and the posed environmental risks. Furfural transformed into a series of halogenated byproducts, despite lower halogen ion concentrations compared to flowback and produced fluids. While halogenated organic byproduct formation is an unintended consequence, they are associated adverse health effects [30]. At elevated pressure, two additional halogenated byproducts were detected. Some halogenated byproducts produced, including bromoform, are known carcinogens and regulated by the EPA in drinking water. Future studies should assess the potential for halogenated organic byproduct formation in hydraulic fracturing brine with elevated halogen concentrations.

Elevated pressure impacted persulfate activation and furfural degradation. During colder months, if persulfate is not activated by temperature, it may be activated downhole by extreme pressures and the risk for halogenated organic byproduct formation still exists. Wellbore conditions play a role in activating persulfate and more information is necessary to understand how persulfate washing impacts surrounding shale formations. As 50% of reported hydraulic fracturing spills are related to fluid storage and transportation [80], understanding additive transformation and awareness of fluid contents at different stages of a fracture is increasingly important. While the industry is still exempt from the Safe Drinking Water Act, this study provides insight into the toxic transformation byproducts that may form in hydraulic fracturing fluids and may be used to help develop methods to safely store, transport, and reuse these fluids.

Acknowledgments

Funding for this project was provided by the Science Alliance, A Tennessee Center for Excellence.

Appendix A. Supplementary data

Supplementary data associated with this article can be found, in the online version, at https://doi.org/10.1016/j.cej.2018.07.142.

References

[1] NOAA/NWS/NCEP/CPC, A. Artusa, D. Bathke, C. Fenimore, B. Fuchs, R. Heim, E. Luebehusen, D. Miskus, B. Rippey, M. Rosencrans, D. Simeral, M. Svoboda, R. Tinker, U.S. Drought Monitor, The National Drought Mitigation Center, Lincoln, NE, 2016.
[2] U.S.EIA, Annual Energy Outlook 2014 with projections to 2040, Washington, DC, 2014.
[3] F.R. Spellman, Environmental Impacts of Hydraulic Fracturing, CRC Press, 2012.
[4] K.B. Gregory, R.D. Vidic, D.A. Dzombak, Water management challenges associated with the production of shale gas by hydraulic fracturing, Elements 7 (2011) 181–186.
[5] R.D. Vidic, S.L. Brantley, J.M. Vandenbossche, D. Yoxtheimer, J.D. Abad, Impact of shale gas development on regional water quality, Science 340 (2013).
[6] W.T. Stringfellow, J.K. Domen, M.K. Camarillo, W.L. Sandelin, S. Borglin, Physical, chemical, and biological characteristics of compounds used in hydraulic fracturing, J. Hazard. Mater. 275 (2014) 37–54.
[7] H. Chen, K.E. Carter, Water usage for natural gas production through hydraulic fracturing in the United States from 2008 to 2014, J. Environ. Manage. 170 (2016) 152–159.
[8] H. Chen, K.E. Carter, Characterization of the chemicals used in hydraulic fracturing fluids for wells located in the Marcellus Shale Play, J. Environ. Manage. 200 (2017) 312–324.
[9] K.E. Manz, K.E. Carter, Investigating the effects of heat activated persulfate on the degradation of furfural, a component of hydraulic fracturing fluid chemical additives, Chem. Eng. J. 327 (2017) 1021–1032.
[10] W.T. Stringfellow, M.K. Camarillo, J.K. Domen, W.L. Sandelin, C. Varadharajan, P.D. Jordan, M.T. Reagan, H. Cooley, M.G. Heberger, J.T. Birkholzer, Identifying chemicals of concern in hydraulic fracturing fluids used for oil production, Environ. Pollut. 220 (2017) 413–420.
[11] K.E. Manz, K.E. Carter, Degradation of hydraulic fracturing additive 2-butoxyethanol using heat activated persulfate in the presence of shale rock, Chemosphere 206 (2018) 398–404.
[12] K.E. Manz, G. Haerr, J. Lucchesi, K.E. Carter, Adsorption of hydraulic fracturing fluid components 2-butoxyethanol and furfural onto granular activated carbon and shale rock, Chemosphere 164 (2016) 585–592.
[13] M.C. McLaughlin, T. Borch, J. Blotevogel, Spills of hydraulic fracturing chemicals on agricultural topsoil: biodegradation, sorption, and co-contaminant interactions, Environ. Sci. Technol. 50 (2016) 6071–6078.
[14] G.A. Kahrilas, J. Blotevogel, E.R. Corrin, T. Borch, Downhole transformation of the hydraulic fracturing fluid biocide glutaraldehyde: implications for flowback and produced water quality, Environ. Sci. Technol. 50 (2016) 11414–11423.
[15] A.O. Aliu, J. Guo, S. Wang, X. Zhao, Hydraulic fracture fluid for gas reservoirs in petroleum engineering applications using sodium carboxy methyl cellulose as gelling agent, J. Nat. Gas Sci. Eng. 32 (2016) 491–500.
[16] C. Liang, Z.-S. Wang, C.J. Bruell, Influence of pH on persulfate oxidation of TCE at ambient temperatures, Chemosphere 66 (2007) 106–113.
[17] H. Liu, T.A. Bruton, W. Li, J.V. Buren, C. Prasse, F.M. Doyle, D.L. Sedlak, Oxidation of benzene by persulfate in the presence of Fe(III)- and Mn(IV)-containing oxides: stoichiometric efficiency and transformation products, Environ. Sci. Technol. 50 (2016) 890–898.
[18] D.A. House, Kinetics and mechanism of oxidations by peroxydisulfate, Chem. Rev. 62 (1962) 185–203.
[19] I.M. Kolthoff, I.K. Miller, The chemistry of persulfate. I. The kinetics and mechanism of the decomposition of the persulfate ion in aqueous medium1, J. Am. Chem. Soc. 73 (1951) 3055–3059.
[20] A. Tsitonaki, B. Petri, M. Crimi, H. MosbÆK, R.L. Siegrist, P.L. Bjerg, In situ chemical oxidation of contaminated soil and groundwater using persulfate: a review, Crit. Rev. Environ. Sci. Technol. 40 (2010) 55–91.
[21] P. Neta, R.E. Huie, A.B. Ross, Rate constants for reactions of inorganic radicals in aqueous solution, J. Phys. Chem. Ref. Data 17 (1988) 1027–1284.
[22] H. Liu, T.A. Bruton, F.M. Doyle, D.L. Sedlak, In situ chemical oxidation of contaminated groundwater by persulfate: decomposition by Fe(III)- and Mn(IV)-containing oxides and aquifer materials, Environ. Sci. Technol. 48 (2014) 10330–10336.
[23] M.L. Hladik, M.J. Focazio, M. Engle, Discharges of produced waters from oil and gas extraction via wastewater treatment plants are sources of disinfection by-products to receiving streams, Sci. Total Environ. 466–467 (2014) 1085–1093.
[24] K.M. Parker, T. Zeng, J. Harkness, A. Vengosh, W.A. Mitch, Enhanced formation of disinfection byproducts in shale gas wastewater-impacted drinking water supplies, Environ. Sci. Technol. 48 (2014) 11161–11169.
[25] J.S. Harkness, G.S. Dwyer, N.R. Warner, K.M. Parker, W.A. Mitch, A. Vengosh, Iodide, bromide, and ammonium in hydraulic fracturing and oil and gas wastewaters: environmental implications, Environ. Sci. Technol. 49 (2015) 1955–1963.
[26] K. Hoelzer, A.J. Sumner, O. Karatum, R.K. Nelson, B.D. Drollette, M.P. O'Connor, E.L. D'Ambro, G.J. Getzinger, P.L. Ferguson, C.M. Reddy, M. Elsner, D.L. Plata, Indications of transformation products from hydraulic fracturing additives in shale-gas wastewater, Environ. Sci. Technol. 50 (2016) 8036–8048.
[27] J. Lu, J. Wu, Y. Ji, D. Kong, Transformation of bromide in thermo activated persulfate oxidation processes, Water Res. 78 (2015) 1–8.
[28] E.E. Yost, J. Stanek, L.D. Burgoon, A decision analysis framework for estimating the potential hazards for drinking water resources of chemicals used in hydraulic fracturing fluids, Sci. Total Environ. (2016).
[29] USEPA, Stage 1 and Stage 2 Disinfectants and Disinfection Byproducts Rules.
[30] S.D. Richardson, J.E. Simmons, G. Rice, Peer reviewed: disinfection byproducts: the next generation, Environ. Sci. Technol. 36 (2002) 198A–205A.
[31] S. Snyder, Water scarcity–the US connection, Afr. J. Food Agric. Nutr. Dev. 14 (2014) 14–15.
[32] N. Devineni, U. Lall, E. Etienne, D. Shi, C. Xi, America's water risk: current demand and climate variability, Geophys. Res. Lett. 42 (2015) 2285–2293.
[33] N.E. Lauer, J.S. Harkness, A. Vengosh, Brine spills associated with unconventional oil development in North Dakota, Environ. Sci. Technol. 50 (2016) 5389–5397.
[34] E.W. Boyer, B.R. Swistock, J. Clark, M. Madden, D.E. Rizzo, The impact of Marcellus gas drilling on rural drinking water supplies, 2012.
[35] E.W. Boyer, B.R. Swistock, J. Clark, M. Madden, D.E. Rizzo, The impact of Marcellus gas drilling on rural drinking water supplies, 2012.
[36] D. Rahm, Regulating hydraulic fracturing in shale gas plays: the case of Texas, Energy Policy 39 (2011) 2974–2981.
[37] K.L. Hickenbottom, N.T. Hancock, N.R. Hutchings, E.W. Appleton, E.G. Beaudry, P. Xu, T.Y. Cath, Forward osmosis treatment of drilling mud and fracturing wastewater from oil and gas operations, Desalination 312 (2013) 60–66.
[38] C. Liang, Z.-S. Wang, N. Mohanty, Influences of carbonate and chloride ions on

persulfate oxidation of trichloroethylene at 20 °C, Sci. Total Environ. 370 (2006) 271–277.
[39] R.E. Huie, C.L. Clifton, Rate constants for hydrogen abstraction reactions of the sulfate radical, SO4−. Alkanes and ethers, Int. J. Chem. Kinetics 21 (1989) 611–619.
[40] J. Kiwi, A. Lopez, V. Nadtochenko, Mechanism and kinetics of the OH-radical intervention during fenton oxidation in the presence of a significant amount of radical scavenger (Cl-), Environ. Sci. Technol. 34 (2000) 2162–2168.
[41] L.R. Bennedsen, J. Muff, E.G. Søgaard, Influence of chloride and carbonates on the reactivity of activated persulfate, Chemosphere 86 (2012) 1092–1097.
[42] J.D. Arthur, B. Bohm, M. Layne, Hydraulic fracturing considerations for natural gas wells of the Marcellus Shale, (2009).
[43] V. Marcon, C. Joseph, K.E. Carter, S.W. Hedges, C.L. Lopano, G.D. Guthrie, J.A. Hakala, Experimental insights into geochemical changes in hydraulically fractured Marcellus Shale, Appl. Geochem. 76 (2017) 36–50.
[44] J. Ma, H. Li, L. Chi, H. Chen, C. Chen, Changes in activation energy and kinetics of heat-activated persulfate oxidation of phenol in response to changes in pH and temperature, Chemosphere 189 (2017) 86–93.
[45] A. Ghauch, A. Baalbaki, M. Amasha, R. El Asmar, O. Tantawi, Contribution of persulfate in UV-254nm activated systems for complete degradation of chloramphenicol antibiotic in water, Chem. Eng. J. 317 (2017) 1012–1025.
[46] B. Legarth, E. Huenges, G. Zimmermann, Hydraulic fracturing in a sedimentary geothermal reservoir: results and implications, Int. J. Rock Mech. Min. Sci. 42 (2005) 1028–1041.
[47] H.A. Waxman, E.J. Markey, D. DeGette, Chemicals used in hydraulic fracturing, United States House of Representatives Committee on Energy and Commerce Minority Staff (2011).
[48] M. Zoveidavianpoor, A. Gharibi, Application of polymers for coating of proppant in hydraulic fracturing of subterraneous formations: a comprehensive review, J. Nat. Gas Sci. Eng. 24 (2015) 197–209.
[49] K.E. Manz, K.E. Carter, Extraction and recovery of 2-butoxyethanol from aqueous phases containing high saline concentration, Anal. Chem. Res. 9 (2016) 1–7.
[50] E.E. Yost, J. Stanek, R.S. DeWoskin, L.D. Burgoon, Overview of chronic oral toxicity values for chemicals present in hydraulic fracturing fluids, flowback, and produced waters, Environ. Sci. Technol. 50 (2016) 4788–4797.
[51] A.R. Hendrickson, R.B.R. Dowell, D.R. Wieland, Acid Reaction Parameters and Reservoir Characteristics Used in the Design of Acidizing Treatments, Society of Petroleum Engineers.
[52] C. Liang, H.-W. Su, Identification of sulfate and hydroxyl radicals in thermally activated persulfate, Ind. Eng. Chem. Res. 48 (2009) 5558–5562.
[53] A. Ghauch, A.M. Tuqan, N. Kibbi, Ibuprofen removal by heated persulfate in aqueous solution: a kinetics study, Chem. Eng. J. 197 (2012) 483–492.
[54] C. Zhu, F. Zhu, D.D. Dionysiou, D. Zhou, G. Fang, J. Gao, Contribution of alcohol radicals to contaminant degradation in quenching studies of persulfate activation process, Water Res. 139 (2018) 66–73.
[55] M. Leili, G. Moussavi, K. Naddafi, Degradation and mineralization of furfural in aqueous solutions using heterogeneous catalytic ozonation, Desalin. Water Treat. 51 (2013) 6789–6797.
[56] A. Nezamzadeh-Ejhieh, S. Moeinirad, Heterogeneous photocatalytic degradation of furfural using NiS-clinoptilolite zeolite, Desalination 273 (2011) 248–257.
[57] R. Boopathy, H. Bokang, L. Daniels, Biotransformation of furfural and 5-hydroxymethyl furfural by enteric bacteria, J. Ind. Microbiol. 11 (1993) 147–150.
[58] C. Liang, C.-F. Huang, N. Mohanty, R.M. Kurakalva, A rapid spectrophotometric determination of persulfate anion in ISCO, Chemosphere 73 (2008) 1540–1543.
[59] L. Levitt, B.W. Levitt, Kinetics and mechanism of the persulphate oxidation of 2-propanol and 2-butanol, Can. J. Chem. 41 (1963) 209–214.
[60] K.-C. Huang, R.A. Couttenye, G.E. Hoag, Kinetics of heat-assisted persulfate oxidation of methyl tert-butyl ether (MTBE), Chemosphere 49 (2002) 413–420.
[61] S.V. Golikeri, D. Luss, Analysis of activation energy of grouped parallel reactions, AIChE J. 18 (1972) 277–282.
[62] T. Wang, T. Kadlac, R. Lenahan, Persistence of fenthion in the aquatic environment, Bull. Environ. Contamination Toxicol. 42 (1989) 389–394.
[63] I. Kaur, R.P. Mathur, S.N. Tandon, P. Dureja, Persistence of endosulfan (technical) in water and soil, Environ. Technol. 19 (1998) 115–119.
[64] M.I. Badawy, M.A. El-Dib, Persistence and fate of methyl parathion in sea water, Bull. Environ. Contamination Toxicol. 33 (1984) 40–49.
[65] R.L. Johnson, P.G. Tratnyek, R.O.B. Johnson, Persulfate persistence under thermal activation conditions, Environ. Sci. Technol. 42 (2008) 9350–9356.
[66] A. Ghauch, A.M. Tuqan, Oxidation of bisoprolol in heated persulfate/H2O systems: kinetics and products, Chem. Eng. J. 183 (2012) 162–171.
[67] X.-R. Xu, X.-Z. Li, Degradation of azo dye Orange G in aqueous solutions by persulfate with ferrous ion, Sep. Purif. Technol. 72 (2010) 105–111.
[68] G.P. Anipsitakis, D.D. Dionysiou, M.A. Gonzalez, Cobalt-mediated activation of peroxymonosulfate and sulfate radical attack on phenolic compounds. Implications of chloride ions, Environ. Sci. Technol. 40 (2006) 1000–1007.
[69] G.R. Aiken, Chloride interference in the analysis of dissolved organic carbon by the wet oxidation method, Environ. Sci. Technol. 26 (1992) 2435–2439.
[70] A. Ghauch, A.M. Tuqan, N. Kibbi, Naproxen abatement by thermally activated persulfate in aqueous systems, Chem. Eng. J. 279 (2015) 861–873.
[71] G.R. Peyton, The free-radical chemistry of persulfate-based total organic carbon analyzers, Mar. Chem. 41 (1993) 91–103.
[72] H. Sato, F. Hirata, Theoretical study for autoionization of liquid water: temperature dependence of the ionic product (pKw), J. Phys. Chem. A 102 (1998) 2603–2608.
[73] N. Yoshida, R. Ishizuka, H. Sato, F. Hirata, Ab initio theoretical study of temperature and density dependence of molecular and thermodynamic properties of water in the entire fluid region: autoionization processes, J. Phys. Chem. B 110 (2006) 8451–8458.
[74] R. Vácha, V. Buch, A. Milet, J.P. Devlin, P. Jungwirth, Autoionization at the surface of neat water: is the top layer pH neutral, basic, or acidic? PCCP 9 (2007) 4736–4747.
[75] A.V. Bandura, S.N. Lvov, The ionization constant of water over wide ranges of temperature and density, J. Phys. Chem. Ref. Data 35 (2005) 15–30.
[76] O.S. Furman, A.L. Teel, R.J. Watts, Mechanism of base activation of persulfate, Environ. Sci. Technol. 44 (2010) 6423–6428.
[77] E. Barbot, N.S. Vidic, K.B. Gregory, R.D. Vidic, Spatial and temporal correlation of water quality parameters of produced waters from devonian-age shale following hydraulic fracturing, Environ. Sci. Technol. 47 (2013) 2562–2569.
[78] L.O. Haluszczak, A.W. Rose, L.R. Kump, Geochemical evaluation of flowback brine from Marcellus gas wells in Pennsylvania, USA, Appl. Geochem. 28 (2013) 55–61.
[79] D. Barceló, Emerging Organic Contaminants and Human Health, Springer, 2012.
[80] L.A. Patterson, K.E. Konschnik, H. Wiseman, J. Fargione, K.O. Maloney, J. Kiesecker, J.-P. Nicot, S. Baruch-Mordo, S. Entrekin, A. Trainor, J.E. Saiers, Unconventional oil and gas spills: risks, mitigation priorities, and state reporting requirements, Environ. Sci. Technol. (2017).